Molecular Dynamics of Variegated Polyamide Dendrimers

Benjamin P. Roberts,[†] Guy Y. Krippner,[‡] Martin J. Scanlon,[†] and David K. Chalmers*[,†]

Medicinal Chemistry and Drug Action, Monash Institute of Pharmaceutical Sciences, 381 Royal Parade, Parkville, Victoria 3052, Australia, and Verva Pharmaceuticals Ltd., PO Box 1069, Grovedale, Victoria 3216, Australia

Received September 23, 2008; Revised Manuscript Received December 17, 2008

ABSTRACT: We have used molecular dynamics simulations to study the structures of a range of heterogeneously functionalized ("variegated") dendrimers and the distributions in space of their caps. By a virtual capping approach, we compare an asymmetric dendrimer (dendritic poly(L-lysine), PLL) and a symmetric polyamide (SPAM) dendrimer. SPAM is larger and more spherical than PLL, and its caps are more evenly distributed throughout the molecule. Protonation of an amine-capped dendrimer causes substantial swelling. The distribution of caps relative to each other is strongly affected by conformational change. Simulation of a SPAM framework with chemically distinct caps shows that whole-dendrimer properties are largely unaffected by the topological arrangement of the caps. Using both modeling approaches, we found that differentiation at the dendrimer's core produces strongly dipolar dendrimers, while differentiation between branches in the outermost generation produces largely nonpolar dendrimers, with a gradual transition between these extremes. The effect of variegation topology on spatial distribution of caps is modified by the interactions between the caps (particularly electrostatic interactions) and with other species in the environment.

Introduction

Dendrimers are highly polyfunctional compounds, consisting of a core, several generations of branching monomers, and with each branch terminated by a capping group. A large proportion of a dendrimer's atoms are contributed by its caps. It has also been shown that a dendrimer's surface is largely composed of caps, even if some caps are located in the dendrimer's interior.[1] The caps play a crucial role in determining the dendrimer's properties and its interaction with the environment. All the earliest dendrimers came with only one kind of cap. Notably, the pioneering syntheses of Vögtle,[2] Newkome,[3] and Tomalia[4] produced homogeneously functionalized dendrimers. In the early 1990s, the development of the convergent synthesis by Fréchet et al.[5−7] provided a relatively straightforward route to dendrimers with different branches attached to the same core. This introduced a new class of dendrimers, which we call variegated dendrimers.[8] The defining characteristic of a variegated dendrimer is that at least one generation of monomers, or the layer of caps, is heterogeneous. Variegated dendrimers have been produced by the convergent synthesis[7,9,10] and by divergent strategies involving orthogonal protection of monomers.[11,12] The possibilities of introducing synergistic functionalities or creating binding sites on the dendrimer's surface are intriguing, and variegated dendrimers have been explored for use in a variety of applications, for example as dendrimer-assisted gene transfection agents,[13] drug delivery devices,[14] covalently bound prodrugs,[15,16] and nanoscale probes.[17] The effect of variegation on dendrimer structure remains relatively poorly studied. Especially, there are very few reports of structural characterization of variegated dendrimers. Techniques such as nuclear magnetic resonance (NMR) spectroscopy[14,18−20] and mass spectrometry[20,21] have been used to determine the overall level of functionalization[22] but often convey limited information about the relative distribution of functional groups. Walter et al.[23] and Han et al.[24] have used electron paramagnetic resonance (EPR) spectroscopy to study variegated PAMAM dendrimers and conclude that the flexible and dynamic framework structure produces a largely random distribution of different caps about the surface. Likewise, in the field of computer simulation, few studies have been made of variegated dendrimers. Suek and Lamm[25] used molecular dynamics to study dendrimers with mixed solvophobic and solvophilic caps using a coarse-grained model. Lee et al.[26] have simulated PAMAM dendrimers with 90% acetylated chain termini. To improve the prospects of utilizing variegated dendrimers, it is essential to have a good understanding of their structure, especially the effect on the dendrimer's structure and properties of changing the variegation pattern.

The present study uses atomistic molecular dynamics (MD) simulations to investigate the effect of variegation using fourth-generation poly(L-lysine) (PLL) and symmetric polyamide (SPAM) frameworks (Figure 1). PLL dendrimers were first reported in the early 1980s[27,28] and have been explored for diverse uses, such as scaffolds for antigenic peptides[29] and vaccines,[30,31] gene delivery agents,[13,32] and antimicrobial and antiparasitic agents.[33−35] Variegated PLL dendrimers have been proposed as antigenic compounds,[36] as antimicrobial agents,[37] and as drug delivery devices.[37] SPAM dendrimers have been synthesized in solution[38−40] and on solid-phase supports[41] and have been proposed as scaffolds for labels in chemiluminescence,[38] as in vivo molecular transporters,[42] and for other biomedical applications.[37,43]

The fourth-generation PLL and SPAM dendrimers are in many ways similar, being flexible aliphatic polyamide dendrimers and each having 32 capping sites. It is therefore useful to compare these dendrimers. There are several key differences between them, however. The chains comprising the PLL dendrimer cover a wide range of lengths, ranging from 14 to 34 bonds, counting from the carbonyl carbon atom of the core to the cap. By contrast, all chains in the SPAM dendrimer are 32 bonds long, counting from the methylene carbon in the core nearest to any cap. The SPAM dendrimer ($M_r = 6260$ g mol^{-1}) is also larger than the PLL dendrimer ($M_r = 4157$ g mol^{-1}).

In the second part of this work, we use MD simulations of SPAM dendrimers with explicitly represented caps, investigating the effects of cap chemistry. The SPAM dendrimers are functionalized with ammonium and carboxylate caps, or with ammonium and alcohol caps, in several different topological arrangements.

* To whom correspondence should be addressed.
[†] Monash Institute of Pharmaceutical Sciences.
[‡] Verva Pharmaceuticals Ltd.

10.1021/ma8021579 CCC: $40.75
Published on Web 03/18/2009

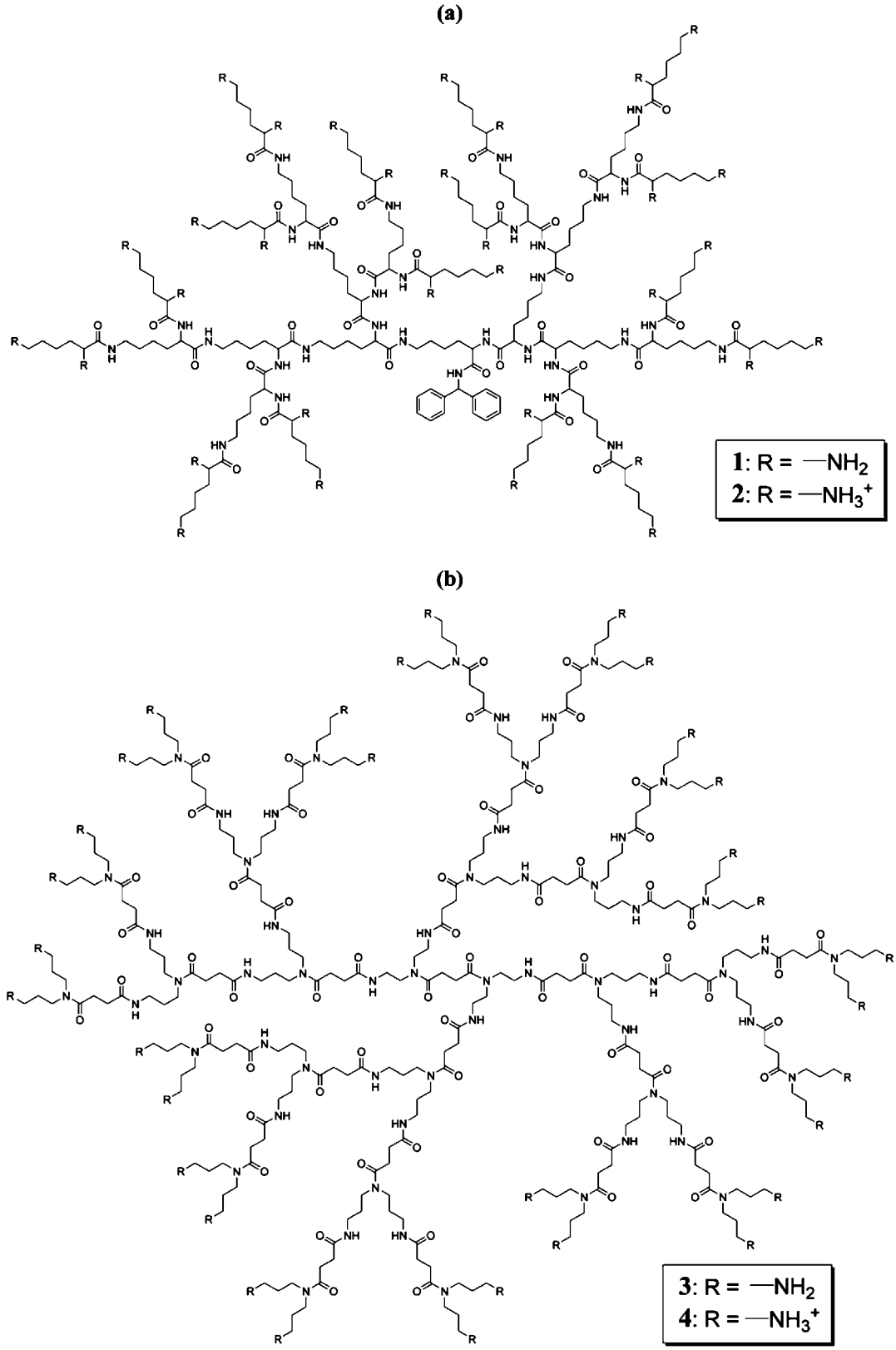

Figure 1. (a) Structure of a fourth-generation poly(L-lysine) (PLL) dendrimer. (b) Structure of a fourth-generation symmetric polyamide (SPAM) dendrimer.

To summarize, this work uses two different approaches to investigate variegation. In the first approach we use virtual capping in conjunction with MD to compare different dendritic frameworks, conformations, and cap topologies, without interference from cap chemistries. In the second approach, presented in the latter part of the paper, caps are represented explicitly.

Methods

The simulations described in this paper were carried out using the protocol we described in a previous paper[44] and which we describe here briefly. Dendrimers were built using Starmaker, a dendrimer construction script forming part of our Silico package.[45] After adding each generation of monomers, Starmaker used Sybyl[46]

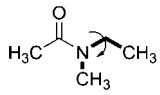

Figure 2. *N*-Ethyl-*N*-methylacetamide, with the parametrized torsion angle shown in bold and indicated by a curved arrow.

and the Tripos force field[47] to perform energy minimization, reducing the risk of atom overlaps in the completed dendrimer. Randomized initial configurations were generated as needed from an extended structure produced by Starmaker, using the Silico script *randomise_conformation*, which rotates the torsion angles of at least 100 appropriate single bonds by arbitrary amounts, minimizing the energy of the output structure in Sybyl.[46] For each dendrimer studied using the virtual cap approach we produced two randomized conformations, in addition to one conformation from the compression protocol. Randomized conformations are compressed to a significant extent by the randomization process and were not compressed further.

Except for the initial dendrimer construction and randomization steps, all energy minimizations and MD simulations used the OPLS-AA force field.[48−54] We provided parameters for the benzhydrylamide core (described in our earlier work[44]) and for the torsion of the alkyl chains in tertiary amides (C−C−N−C). This torsion is shown in Figure 2. To determine the Fourier coefficients for this torsion, we fitted the OPLS-AA potential energies of *N*-ethyl-*N*-methylacetamide against potential energies computed in Gaussian 98[55] using the MP2 and CCSD(T) methods. The calculated Fourier coefficients for this torsion are $V_1 = 7.4858$, $V_2 = 0.3050$, and $V_3 = 0.0000$.

Each dendrimer was simulated in a (64 Å × 64 Å × 64 Å) cubic periodic cell. Explicit water molecules, represented using the TIP3P model,[56] were added to this cell to a density of 1 g cm^{-3}, along with sodium and chloride ions; the more numerous ion was added at a concentration of 1 M and the less numerous ion until the system was electrically neutral.

Molecular dynamics simulations were performed using NAMD[57,58] version 2.6. The dendrimers were equilibrated by energy minimization, followed by four cycles of constant-volume simulated annealing, each ∼2 ns long (100 ps of heating to 600 K, followed by 1.9 ns of cooling to 300 K), for a total of 8 ns, and an equilibration period of at least 2 ns using an NPT ensemble. Production MD consisted of 10 ns of simulation at 300 K under an NPT ensemble, except one simulation which used the NVE ensemble. For all simulations, a multiple time-stepping protocol was used. In simulated annealing and NPT simulations, bonding interactions were evaluated every time step, short-range nonbonding interactions every second time step, and long-range electrostatics every fourth time step. Under an NVE ensemble, bonding and short-range nonbonding interactions were evaluated every time step and long-range electrostatics every third time step.

Simulation frames were produced from the output trajectories using the program VMD.[59] PyMOL[60] was used for display and graphical rendering, Silico[45] for simulation analysis, and NACCESS,[61] with a Silico wrapper script, for calculation of solvent-accessible surface areas. Radii of gyration, asphericities, congregation coefficients, radial density profiles, and solvent-accessible surface areas were calculated as described previously.[44] For asphericity, we used the definition of Rudnick and Gaspari,[62] based on the eigenvalues of a dendrimer's shape ellipsoid. Asphericity may take a value between 0 (completely spherical) and 1 (completely linear). The congregation coefficient is a measure of the populations of caps in different spherical sectors and may take values between 0 (perfectly dispersed caps) and 1 (perfectly congregated caps). The definition of the congregation coefficient and the procedure for calculating it are set out in our earlier work.[44]

Results and Discussion

Dendrimer Models Using Virtual Caps. The presentation of a dendrimer's caps to the surrounding environment depends on the structure and conformation of the framework, the topological arrangement of caps (the variegation pattern), and the intercap interactions. In this first section of work, we reduce the complexity of this system by simulating homogeneously functionalized dendrimers — where all cap−cap interactions are identical — and applying virtual variegation patterns to these chemically sensible frameworks. Thus, we separate the effects of a change in the framework from those of a change in the variegation pattern.

Even for a small dendrimer, there are very many possible variegation patterns. If a fourth-generation PLL dendrimer is capped with 16 of each of two types of cap, there are more than 6×10^8 possible arrangements. Because of the symmetry of the SPAM dendrimer, most of its variegation patterns are equivalent by rotation; even so, with 16 of each of two types of cap, it has 2682 unique variegation patterns. To simplify this combinatorial problem, we have chosen the subset of variegation patterns which involve 16 of each of two types of cap and are regular variegation patterns. These can be described using the Dotted-Cap Notation,[8] as shown in Figure 3. A variegation pattern is regular if chains are differentiated in a single generation, for example by incorporation into the dendrimer of one perfect generation of orthogonally protected monomers. A regularly variegated dendrimer is said to be variegated on a certain generation; so, for example, in PLL, pattern II is variegated on the first generation and pattern V on the fourth generation. By extension, variegation can be described as on the core, near the core (e.g., on the first generation), or far from the core (e.g., on the fourth generation).

The regular variegation patterns we have investigated are shown in Figure 3. As a simple way to identify caps, when discussing dendrimers with virtual caps, we describe sets of caps as "blue" or "gold" based on their color in Figure 3. When analyzing the results of the simulations, we distinguished between branches on the basis of short or long branches (for PLL dendrimers) or *Z* or *E* stereochemistry (for SPAM dendrimers).

To investigate the effect of symmetric and asymmetric frameworks on the distribution of caps, we simulated the PLL and SPAM frameworks, each in two protonation states, i.e., neutral terminal amino groups and fully protonated terminal amino groups. Simulations were conducted using an NPT ensemble. A single NVE simulation was used to validate the NPT simulations (see Supporting Information). Four systems were modeled (**1**−**4**), which are shown in Figure 1. We expect that at neutral pH a polyamine dendrimer will adopt a protonation state between these two extremes, as other polyamines have been shown to do.[63] These dendrimers should therefore exhibit properties intermediate between the two protonation states. To improve the coverage of conformational space, we carried out three independent simulations of each dendrimer system, each starting from a randomly generated conformation.

Figure 4 shows initial and final snapshots for conformation 3 of dendrimers **1** to **4**. The key difference between the neutral and protonated states is the extension of the branches. Dendrimers **1** and **3** are compressed, with flexible chains which fold back into the interior of the dendrimer. Dendrimers **2** and **4** are highly extended, with most chains pointing away from the core of the dendrimer and from each other.

We used system energies and solvent-accessible surface areas to monitor the systems for equilibration. System energies are stable, as are solvent-accessible surface areas; we conclude that the dendrimers are equilibrated by the start of production MD. Protonation increases the solvent-accessible surface area by 30−50%, and the SPAM dendrimer has a surface area 30−50% larger than the PLL dendrimer.

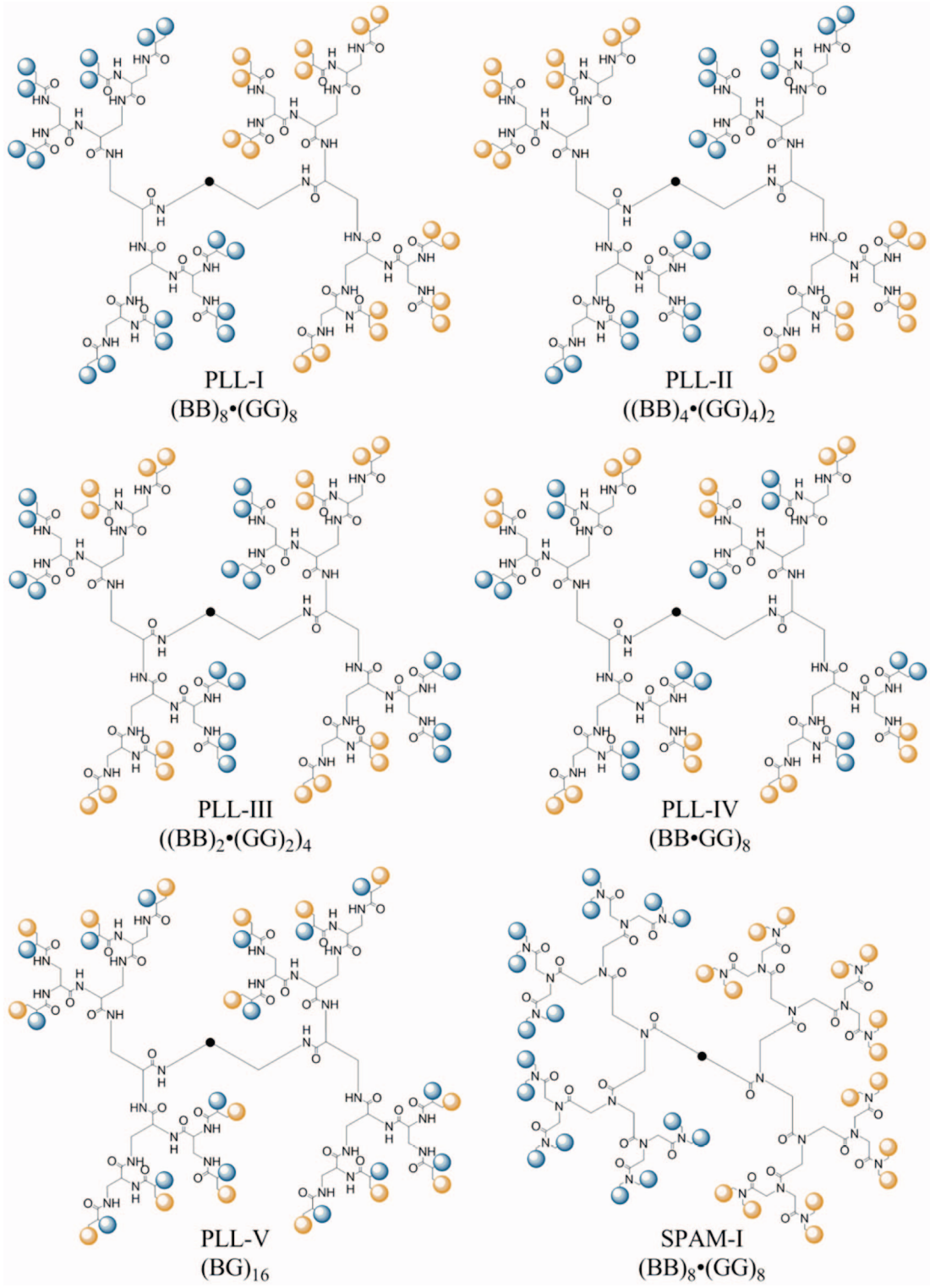

Figure 3. Schematic diagram of variegation patterns for PLL dendrimers (PLL-I−PLL-V). Caps are shown as blue or gold spheres. The dendrimer's core is shown as a black circle. The first variegation pattern for the SPAM dendrimer, SPAM-I, is also shown; SPAM-II−SPAM-V may be envisaged from their PLL equivalents. We also show the descriptors for the patterns according to the Dotted-Cap Notation.[8]

We use the mean-squared radius of gyration (R_g^2), shown in Figure 5, to compare the sizes of the different frameworks, and for each framework, the effects of protonation and conformational change. The mean R_g^2 for the SPAM framework is between 20% and 40% greater than for an equivalently protonated PLL framework. This is expected, given the SPAM framework's greater molecular weight and longer average chain length; Rissanou et al.[64] have previously described a positive correlation between chain length and radius of gyration.

Protonation of the framework leads to significant structural changes. Protonation of the SPAM dendrimer produces an increase in R_g^2 of ∼40%; in the case of the PLL dendrimer, R_g^2 increases by more than 60%. This tendency of the radius of gyration to increase with protonation has been reported in earlier

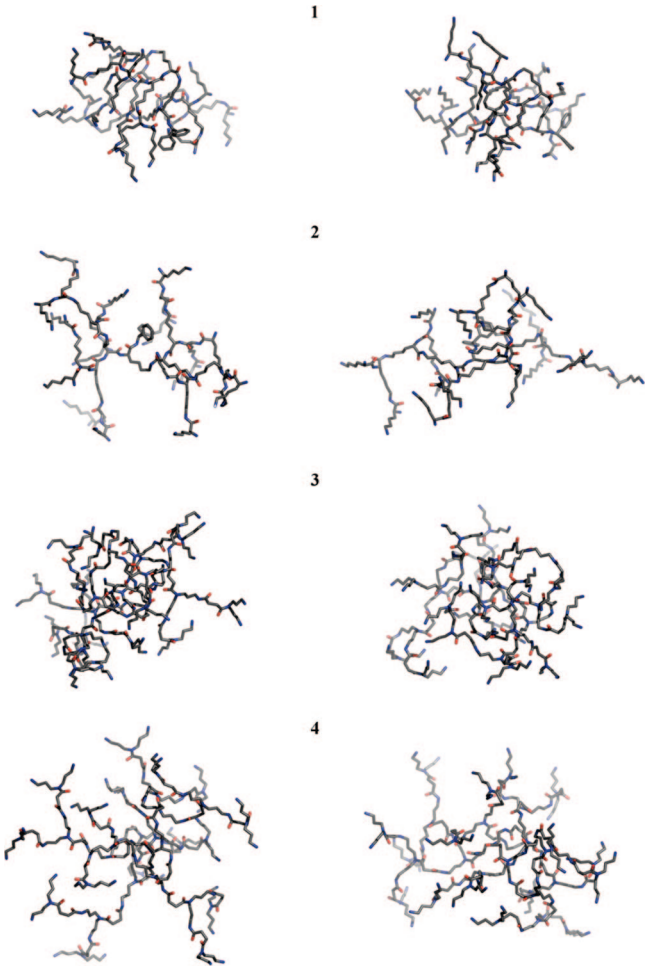

Figure 4. Snapshots of initial (left) and final (right) conformations, from the MD simulations, of the neutral (**1**) and protonated (**2**) PLL dendrimers, and the neutral (**3**) and protonated (**4**) SPAM dendrimers. For each dendrimer, one of the two randomized conformations is shown.

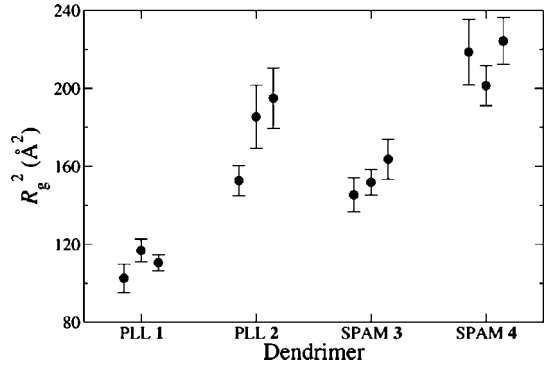

Figure 5. Mean-squared radii of gyration (R_g^2) of the dendrimer frameworks **1**−**4**. Two protonation states are shown for each framework: PLL (**1**, **2**) and SPAM (**3**, **4**). For each protonation state, three simulations, each from a different initial conformation, are shown as separate points. Error bars indicate one standard deviation each side of the mean.

studies.[65−67] Meanwhile, R_g^2 is more variable when the dendrimer is protonated than when it is neutral, as can be seen by the standard deviations (shown by error bars in Figure 5). The protonated dendrimers are also considerably more flexible than their neutral counterparts.

We characterize the shape of the PLL and SPAM dendrimers by calculating the asphericity (Figure 6). Like the radius of

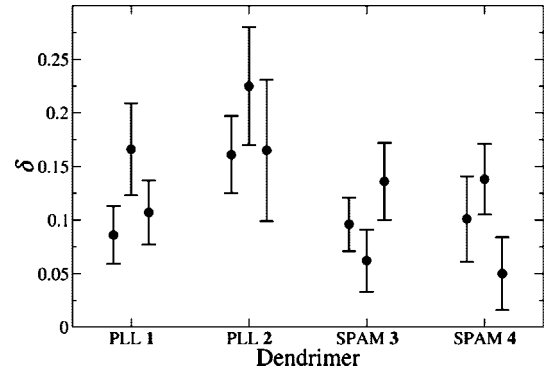

Figure 6. Asphericities (δ) of the dendrimer frameworks **1**−**4**. Two protonation states are shown for each framework: PLL (**1**, **2**) and SPAM (**3**, **4**). For each protonation state, three simulations, each from a different initial conformation, are shown as separate points. Error bars indicate one standard deviation each side of the mean.

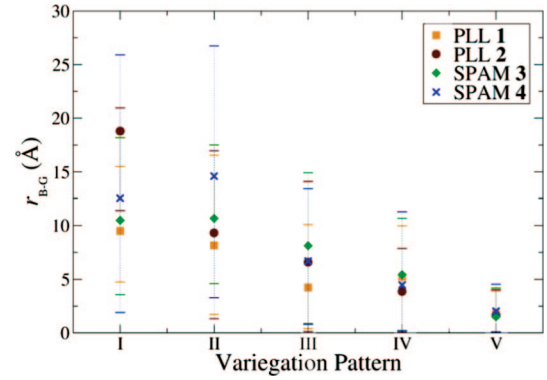

Figure 7. Blue cap−gold cap separation (r_{B-G}) for dendrimer frameworks **1**−**4**. Points mark the mean separation distance over all snapshots in all three conformations. Error bars indicate the maximum and minimum separation distances across all conformations.

gyration, the asphericity varies significantly from conformation to conformation. The SPAM dendrimers are largely spherical, and protonation does not affect their sphericity. The opposite is true of PLL dendrimers, which are less spherical than their SPAM counterparts, and the asphericity becomes more pronounced when a PLL dendrimer is protonated. A PLL dendrimer, especially a protonated one, exhibits more variability in its asphericity than a SPAM dendrimer. This can be explained by the inherent asymmetry of a PLL framework.

Application of labels to the chain-terminating nitrogen atoms introduces the virtual caps into the dendrimers. We used the Silico[45] script *starlabel* to carry out this labeling.

According to the schematic arrangements in Figure 3, a dendrimer variegated on or near the core will be strongly polar, though the polarity is modified in practice by a three-dimensional shape and dendrimer flexibility. To assess the dendrimer's polarity, in the sense of an asymmetric cap distribution, we calculate the distance between the weighted positions of the two groups of caps:

$$r_{B-G} = \left| \frac{1}{N_G} \sum_g \mathbf{r}_g - \frac{1}{N_B} \sum_b \mathbf{r}_b \right| \quad (1)$$

where r_{B-G} is the distance between the average blue cap position and the average gold cap position, a quantity intimately related to the dendrimer's polarity; N_B and N_G are the numbers of blue and gold caps, respectively; and $\mathbf{r}_b$ and $\mathbf{r}_g$ are the positions of each blue cap b and each gold cap g, respectively. These distances are graphed in Figure 7. Variegation on the core induces a significant degree of polarity, but this polarity is very

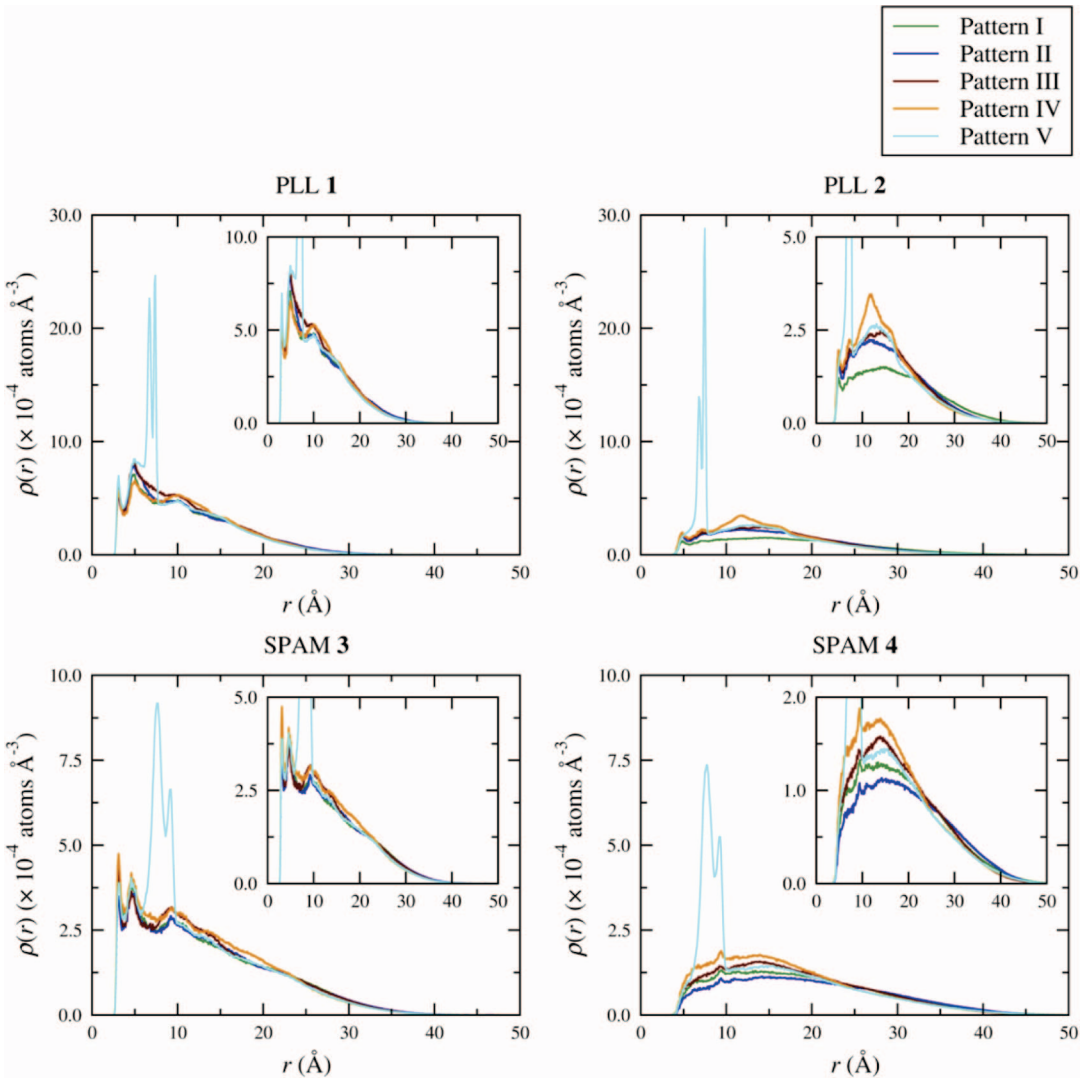

Figure 8. Radial density profiles of all gold caps about blue caps for frameworks **1**−**4** and variegation patterns **I**−**V**. Each distribution is the average of three simulations. Enlargements are shown as insets.

susceptible to conformational changes. There is also a gradual trend toward a nonpolar dendrimer as variegation takes place further from the core, rather than the sudden shift that might be expected, and a simultaneous trend toward reducing the effect of conformational changes on overall polarity. Variegation in the outermost generation, as in PLL-V and SPAM-V, produces a largely nonpolar dendrimer, and this lack of polarity is preserved as the conformation changes. For all variegation patterns, the polarity of PLL dendrimers is similar to that of SPAM dendrimers.

An exciting potential application for dendrimer variegation is the creation of dendrimers with interacting caps or binding sites. Dendrimers with binding sites have been explored, for example, by Delort et al.,[68] who prepared catalytic dendrimers containing multiple histidine caps; Epperson et al.[69] in NMR studies have shown that dendrimer branches can participate in cooperative binding. Since a dendrimer with a variegated surface possesses different caps, the relative distribution of these caps in space, and how this distribution responds to different variegation patterns, is an important question.

We have investigated the distribution of capping sites and how it changes with variegation pattern, using radial density profiles. The radial density profile of gold caps about blue caps is shown in Figure 8. For all variegation patterns, there is a region of high effective gold cap concentration near each blue cap. Pattern V shows striking differences from the other patterns, with a large peak at short distances arising from a cap of the opposite kind attached to the same residue. Patterns I to IV are broadly similar to each other. The distributions for the protonated dendrimers, **2** and **4**, show a mode at between 12 and 15 Å; the radial density of caps at this mode varies by up to 30% as the variegation pattern changes. As the generation where variegation takes place moves away from the core (i.e., the pattern changes from pattern I toward pattern IV), the density of gold caps about blue caps increases at short r and decreases at long r. The neutral dendrimers **1** and **3** also exhibit this behavior but to a lesser extent. At short r, the density of gold caps about blue caps is greater in PLL dendrimers than in SPAM dendrimers, while the reverse is true at $r > 20-25$ Å, as the SPAM framework is larger than the PLL framework.

We have also investigated the distribution of distances from each blue cap to its nearest-neighboring gold cap. This is important for dendrimer design if the aim is to either maximize or minimize the average distance between blue and gold caps (e.g., to produce binding sites). The radial density profiles for blue caps to nearest-neighboring gold cap are shown in Figure 9. As expected, all blue caps are within 10 Å of a gold cap under variegation pattern V, and this is not the case under any of the other variegation patterns. Differences between variegation patterns I−IV are minor, especially when the framework

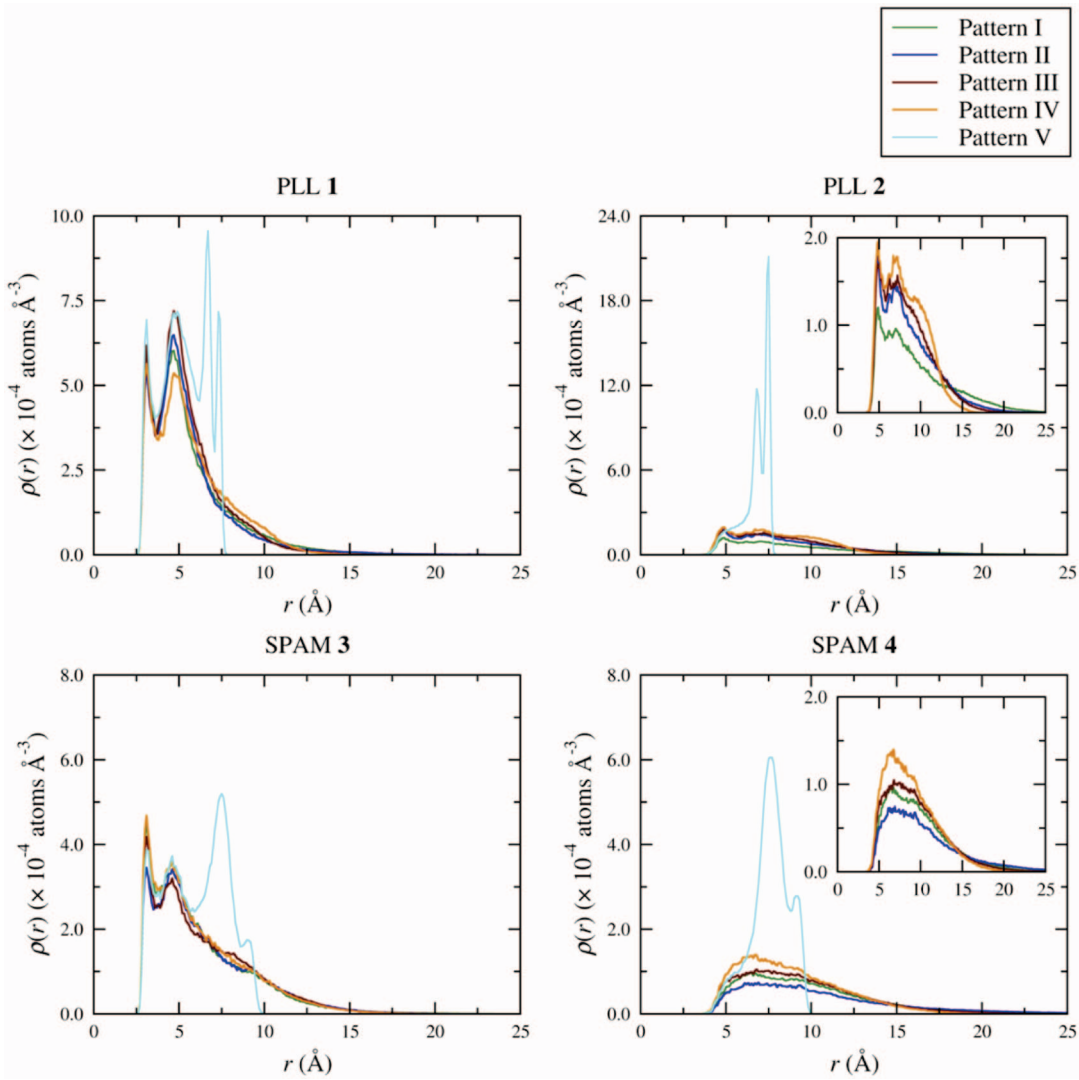

Figure 9. Radial density profiles of the distances between blue caps and their nearest-neighboring gold caps. Density profiles are shown for frameworks **1**−**4** and variegation patterns **I**−**V**. For frameworks 2 and 4, the enlargements show variegation patterns I−IV.

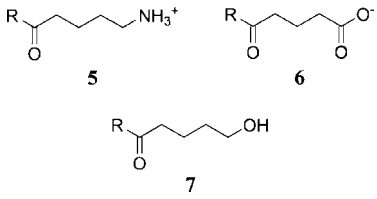

Figure 10. The explicitly represented capping groups used in simulations of variegated dendrimers.

is neutral; if the framework is protonated and the dendrimer is more extended, there is a trend toward more nearest neighbors at short r, and fewer at long r, from pattern I to pattern IV.

To investigate the effect of arbitrarily choosing the blue and gold labels, we have calculated the coefficients of determination (R^2, the squares of the correlation coefficients) between the blue−gold and gold−blue density profiles for our simulations. These coefficients range from 0.9868 (SPAM-II) to 0.9999 (PL-V). This suggests that, in the case of the SPAM dendrimers, we have covered conformational space well. In the case of the PLL dendrimers, while the caps are topologically different, swapping blue caps and gold caps around has no significant effect.

Dendrimers with Explicit, Chemically Distinct Caps. We now discuss the effects of functionalizing the dendrimer with chemically distinct capping groups which are explicitly represented. The structure of these functionalized dendrimers is affected by any interaction between the two types of cap. In this section, we have studied two series of dendrimers based on the SPAM framework, avoiding the effects of asymmetry in PLL dendrimers.

The SPAM framework uses tertiary amide nitrogen atoms as branch points. On the time scale of our simulations, substituents on these branch points resolve into E and Z branches; however, with an energy barrier of ~30 kJ mol^{-1},[70] rotation about the amide bond is facile at room temperature. As a result, for most applications, all the chain-terminal sites in a perfect SPAM dendrimer are topologically equivalent with respect to the core.

By applying primary alkylammonium (**5**), carboxylic acid (**6**), and primary alcohol (**7**) caps in the variegation patterns SPAM-I to SPAM-V described above (Figure 3), we constructed 10 explicitly capped dendrimers, **8**−**17** (Table 1). These 10 dendrimers were simulated according to the general method described above. For each dendrimer, a single conformation, generated by the compression protocol, was used. Equilibration consisted of four 2 ns cycles of simulated annealing, followed by 12 ns of simulation under an NPT ensemble. A further 10 ns of simulation formed the production dynamics. Graphs of the instantaneous total energy of the systems and the dendrimers'

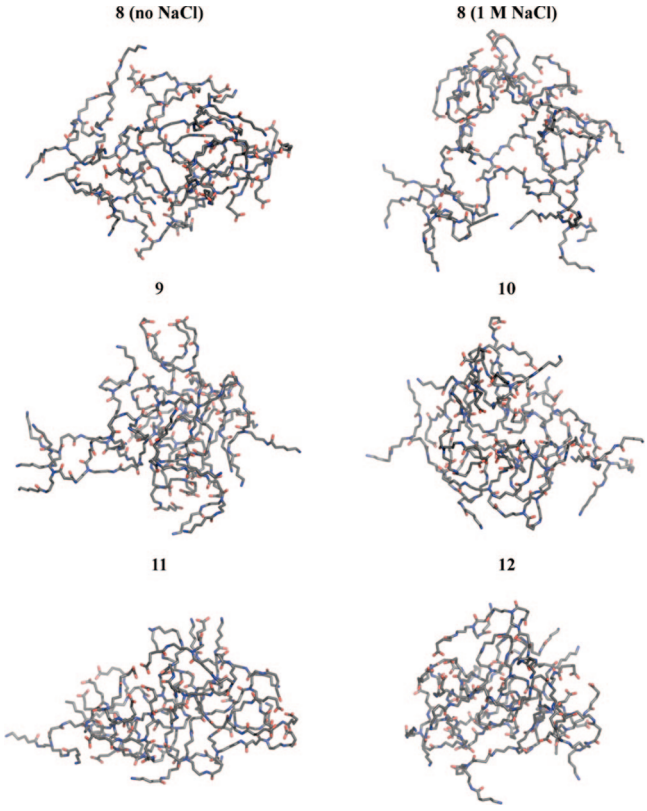

Figure 11. Final snapshots of the simulations of the ammonium/carboxylate capped dendrimers **8** to **12**. (a) is from a simulation of dendrimer **8** in pure water. (b) to (f) are from simulations of dendrimers **8** to **12**, respectively, in 1 M NaCl solution.

Table 1. Arrangements of the Caps on the 10 Simulated Dendrimers with Explicit Differences between Caps

dendrimer	variegation pattern	blue cap	gold cap	R_g (Å)	δ
8	SPAM-I	**5**	**6**	14.8	0.09
9	SPAM-II	**6**	**5**	14.5	0.12
10	SPAM-III	**5**	**6**	14.4	0.06
11	SPAM-IV	**5**	**6**	14.4	0.15
12	SPAM-V	**5**	**6**	13.7	0.06
13	SPAM-I	**5**	**7**	15.4	0.21
14	SPAM-II	**7**	**5**	14.0	0.05
15	SPAM-III	**5**	**7**	13.6	0.07
16	SPAM-IV	**5**	**7**	15.3	0.12
17	SPAM-V	**5**	**7**	13.6	0.06

instantaneous solvent-accessible surface areas are available as Supporting Information.

The final frames of the simulations of these explicitly capped dendrimers are shown in Figure 11 (dendrimers **8**−**12**) and Figure 12 (dendrimers **13**−**17**). The dendrimers largely adopt open conformations, as expected for dendrimers with ionic caps, though not to the same degree as the previously described polycationic frameworks. The ammonium/carboxylate dendrimers, especially **8** and **9**, also exhibit clustering of carboxylate caps when simulated with counterions.

The radii of gyration and asphericities of the dendrimers with mixed ammonium and alcohol caps are shown in Table 1. Comparing dendrimers with the same caps, the radius of gyration varies by more than 10% as the variegation pattern changes. This may correspond to a change in the overall size of the dendrimer or a change to a less isotropic shape. We note that the dendrimers with large R_g (e.g., the ammonium/alcohol capped dendrimers **13** and **16**) also have large asphericities. In the case of **16** in particular, given its open conformation, both effects contribute to a larger R_g. The solvent-accessible surface

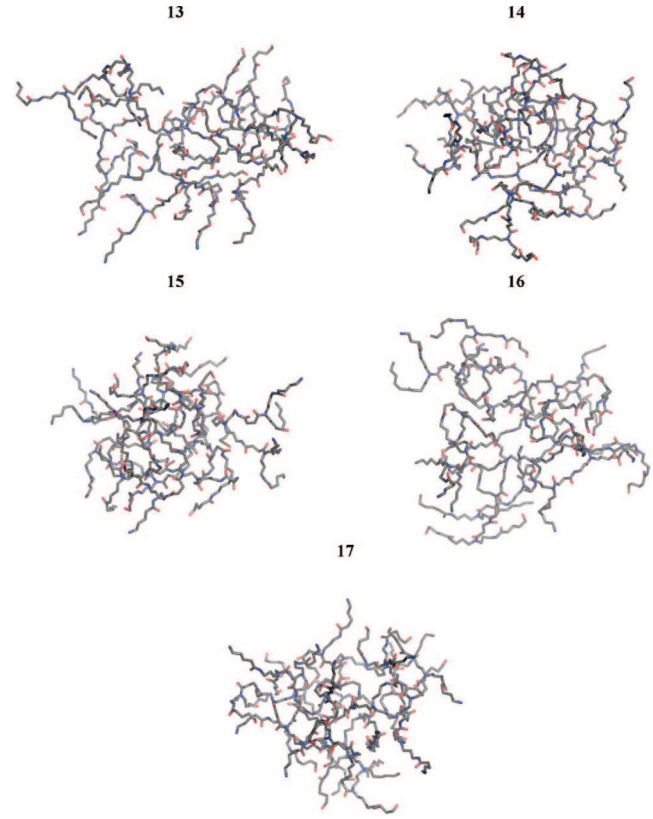

Figure 12. Final snapshots of the simulations of the ammonium/alcohol capped dendrimers **13** (a) to **17** (e).

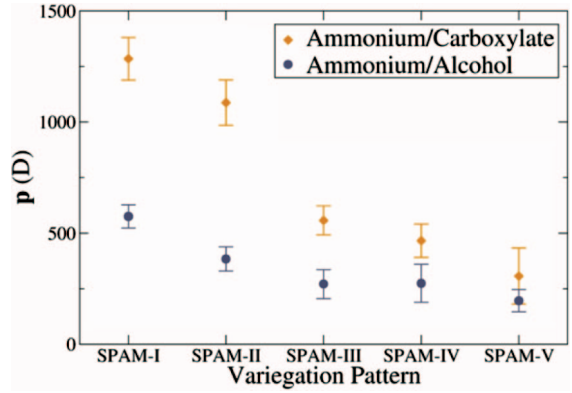

Figure 13. Calculated electrical dipole moments of the ammonium/carboxylate and ammonium/alcohol capped dendrimers.

area is unaffected by the variegation pattern (see Supporting Information).

We calculated electrical dipole moments for the dendrimers **8**−**17** using atomic charges from the OPLS-AA force field. These dipole moments are shown in Figure 13. The dendrimers with variegation pattern I or II are strongly polar, and the magnitude of the dipole moment increases with cap charge. There is a stark difference in polarity between the dendrimers variegated on the core or the first generation and those variegated on the second or more peripheral generations. The magnitude of this effect is greater than was observed for virtually capped dendrimers. The dendrimer with variegation pattern V has a dipole moment close to zero. Variegation on the core is thus an effective way to produce strongly polar dendrimers.

This trend in polarity also indicates a change in the tendency of the two types of cap to associate with each other. We have investigated the association between ammonium and carboxylate caps, or ammonium and alcohol caps, using radial density

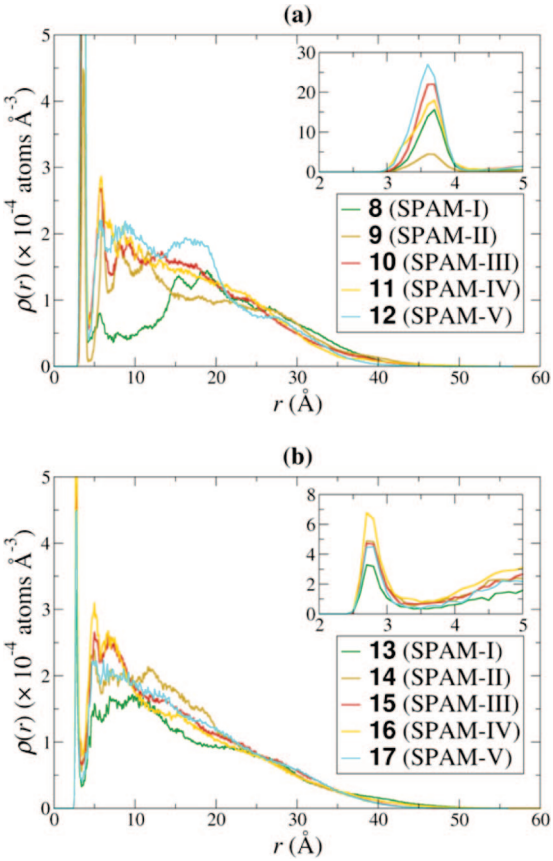

Figure 14. Radial density profiles of (a) ammonium groups about carboxylate groups (dendrimers **8**−**12**) and (b) ammonium groups about alcohol groups (dendrimers **13**−**17**).

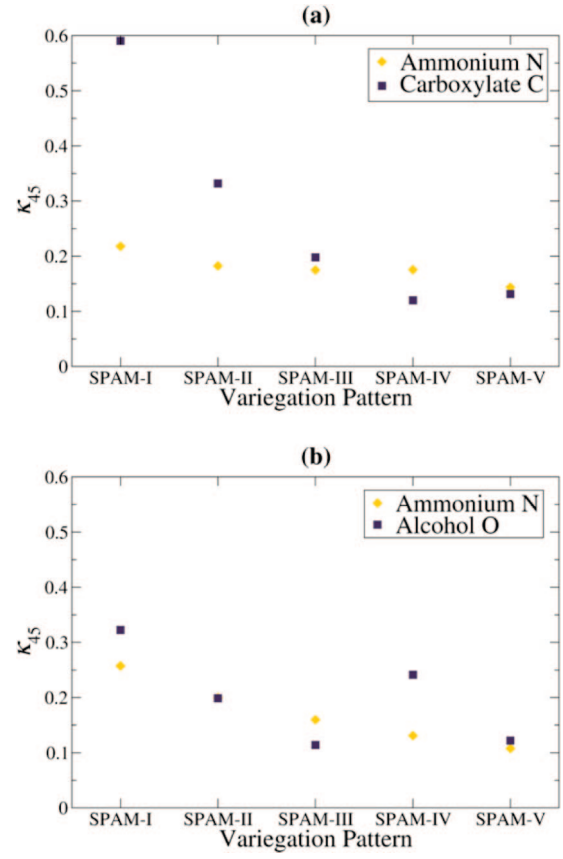

Figure 15. Congregation coefficients of selected atoms in the two different groups of caps in (a) ammonium/carboxylate dendrimers **8** to **12** and (b) ammonium/alcohol dendrimers **13** to **17**.

profiles, which are shown in Figure 14. Variegation on or near the core, as in dendrimers **8** and **9**, decreases the association between ammonium and carboxylate caps. This effect is also present in dendrimer **13**, in which the ammonium and alcohol caps are variegated on the core and associate slightly less with each other than they do when variegated on other generations.

Another property of interest is the extent to which caps of the same kind associate with each other, especially since this is a measure of cooperative behavior. We have represented the extent of congregation of each kind of cap using the congregation coefficient for 45° spherical sectors, κ_{45}. The congregation coefficients for the ammonium/carboxylate and ammonium/alcohol dendrimers are shown in Figure 15. The ammonium and alcohol caps are always largely dispersed and become more so as the variegation pattern moves from I through to V, a process which is forced by the changing cap topology. Even when ammonium caps are arranged according to variegation pattern I, their congregation is discouraged by their positive charges. For the carboxylate groups, there is a much greater decrease in congregation as the variegation pattern changes: when the carboxylate groups are arranged on one side of the dendrimer molecule (e.g., in variegation pattern I), they are largely congregated together, with a congregation coefficient of $\kappa_{45} \approx 0.6$. This suggests an attractive force which is comparable in strength to electrostatic repulsion.

The attractive force between carboxylate groups results from chelation of sodium ions by these groups. Chelation of chloride ions by ammonium groups, by contrast, is not observed. Figure 16 shows the effect of counterions using the final frames of simulations with and without NaCl. When salt is present, the carboxylate groups congregate around clusters of Na^+ ions; in the absence of salt, while the carboxylate groups are still found largely in one-half of the dendrimer — a result of topology — they do not noticeably cluster together.

Some ensemble-averaged properties of dendrimer **8** in the absence and presence of counterions — the radius of gyration (R_g), the asphericity (δ), the 45° congregation coefficient (κ_{45}), and the dipole moment (**p**) — are given in Table 2. As the salt counterions condense onto the dendrimer, they induce swelling, an effect which has been described in earlier reports;[67,71] as a result, the dendrimer becomes both larger and more spherical. Meanwhile, similar caps cluster together much more, as evidenced by the congregation coefficients and the dipole moment, which more than doubles in size.

As shown by the radial density profiles (Figure 17), when salt is added to the simulation, there is an approximately 6-fold decrease in ammonium−carboxylate interaction. This is a result of competition for ionic binding, so addition of salt accentuates the polarity of core-variegated dendrimers where caps are oppositely charged, while in the absence of salt this polarity is suppressed.

Conclusions

This work shows that distribution of dendrimer caps in variegated dendrimers is dependent on the conformation of a flexible PLL or SPAM framework, the topological arrangement of the caps, and their chemical nature. Gross features of the dendrimer such as size and shape are unaffected by the variegation pattern. In general, we find that the SPAM framework is larger and more spherical than PLL, and the caps in a SPAM dendrimer are more evenly spread than caps in PLL. Protonation on terminal nitrogen atoms causes the dendrimer to causes the dendrimer to expand.

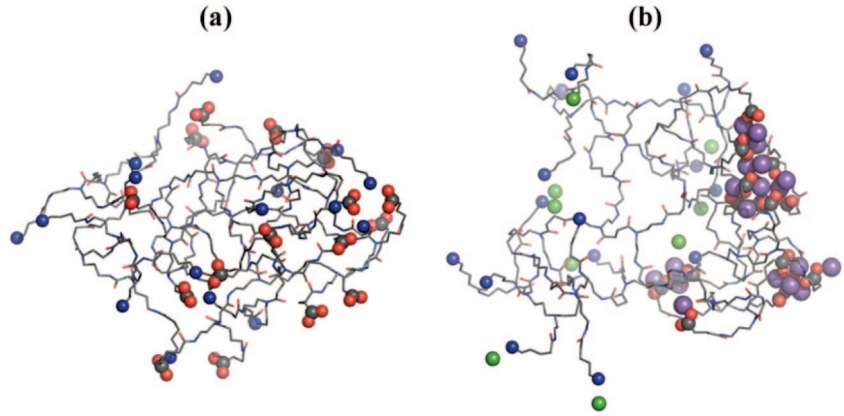

Figure 16. (a) Dendrimer **8** with close ions, as simulated in 1 M aqueous NaCl. (b) Same dendrimer, as simulated in pure water. Carboxylate caps are shown as collections of one dark gray and two red spheres and ammonium caps as individual blue spheres. Sodium ions within 4 Å of a carboxylate cap are shown as purple spheres and chloride ions within 4 Å of an ammonium cap as green spheres. Other dendrimer atoms (except hydrogen atoms) are shown as lines.

Table 2. Some Ensemble-Averaged Properties of the Ammonium/Carboxylate Capped Dendrimer 8, in the Absence and Presence of NaCl Counterions[a]

property	**8** (no NaCl)	**8** (1 M NaCl)
R_g (Å)	14.45	14.78
δ	0.136	0.093
κ_{45} (ammonium N)	0.129	0.218
κ_{45} (carboxylate C)	0.283	0.590
p (D)	480	1285

[a] Radius of gyration, asphericity, 45° congregation coefficients of ammonium and carboxylate groups, and electric dipole moment.

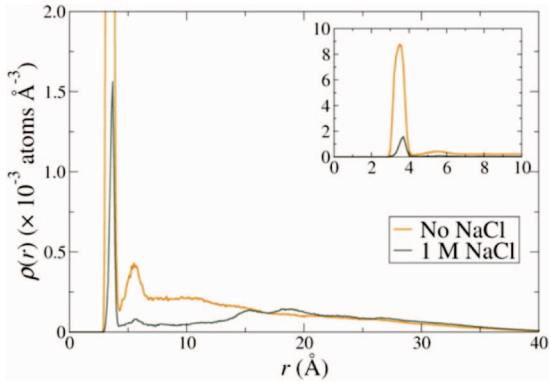

Figure 17. Radial density profile of ammonium caps about carboxylate caps in the dendrimer **8** (variegated on the core), in the absence and presence of 1 M NaCl.

Variegation on the core or the first generation produces strongly dipolar dendrimers and is a reliable way to position similar caps close together in space if the aim is to provide cooperative activity or interaction between caps. Positioning caps close together is best achieved by variegating on the outermost generation. Variegation on intermediate generations produces dendrimers with properties between these extremes, but the results of such variegation depend strongly on the instantaneous conformation of the framework.

Our simulations using explicitly modeled caps show that if the capping groups are attracted to one another, a flexible framework permits them to associate. Cap−cap associations distort the cap arrangement away from that predicted by the variegation pattern and toward a more even distribution. This is most important for dendrimers variegated on or near the core, which may be much less polar than predicted from topology alone. Repulsive interactions between caps, as in protonated PLL and SPAM dendrimers, produce a structure similar to the topological ideal of evenly distributed caps. The structure of the dendrimer is also influenced by environmental species, which may compete with intramolecular groups for binding or form new interactions such as chelation.

Acknowledgment. This research was done in collaboration with Starpharma Pty Ltd. and financially supported by an Australian Research Council linkage grant. Simulations were performed on the Monash Sun Grid (MSG) and at the Victorian Partnership for Advanced Computing (VPAC). The authors thank Dr. Brian Salter-Duke for assistance to develop force field parameters.

Supporting Information Available: Instantaneous energies and solvent-accessible surface areas for the third conformers of the PLL and SPAM frameworks and the explicitly capped SPAM dendrimers **8**−**17**; Pdb format structure files for the final frames of dendrimers **1**−**4** and **9**−**17**. This material is available free of charge via the Internet at http://pubs.acs.org.

References and Notes

(1) Rathgeber, S.; Pakula, T.; Urban, V. *J. Chem. Phys.* **2004**, *121*, 3840–3853.
(2) Buhleier, E.; Wehner, W.; Vögtle, F. *Synthesis* **1978**, 155–158.
(3) Newkome, G. R.; Yao, Z.-q.; Baker, G. R.; Gupta, V. K. *J. Org. Chem.* **1985**, *50*, 2003–2004.
(4) Tomalia, D. A.; Baker, H.; Dewald, J.; Hall, M.; Kallos, G.; Martin, S.; Roeck, J.; Ryder, J.; Smith, P. *Polym. J. (Tokyo, Jpn.)* **1985**, *17*, 117–132.
(5) Hawker, C.; Fréchet, J. M. J. *J. Chem. Soc., Chem. Commun.* **1990**, 1010–1013.
(6) Hawker, C. J.; Fréchet, J. M. J. *J. Am. Chem. Soc.* **1990**, *112*, 7638–7647.
(7) Wooley, K. L.; Hawker, C. J.; Fréchet, J. M. J. *J. Am. Chem. Soc.* **1993**, *115*, 11496–11505.
(8) Roberts, B. P.; Krippner, G. Y.; Scanlon, M. J.; Chalmers, D. K. *New J. Chem.* **2008**, *32*, 1543−1554.
(9) Grayson, S. M.; Fréchet, J. M. J. *J. Am. Chem. Soc.* **2000**, *122*, 10335–10344.
(10) Grayson, S. M.; Fréchet, J. M. *Org. Lett.* **2002**, *4*, 3171–3174.
(11) Sivanandan, K.; Vutukuri, D.; Thayumanavan, S. *Org. Lett.* **2002**, *4*, 3751–3753.
(12) Steffensen, M. B.; Simanek, E. E. *Angew. Chem., Int. Ed.* **2004**, *43*, 5178–5180.
(13) Guillot-Nieckowski, M.; Eisler, S.; Diederich, F. *New J. Chem.* **2007**, *31*, 1111–1127.
(14) Fuchs, S.; Kapp, T.; Otto, H.; Schoneberg, T.; Franke, P.; Gust, R.; Schluter, A. D. *Chem.—Eur. J.* **2004**, *10*, 1167–1192.
(15) Patri, A. K.; Majoros, I. J.; Baker, J. R., Jr. *Curr. Opin. Chem. Biol.* **2002**, *6*, 466–471.
(16) Majoros, I. J.; Thomas, T. P.; Mehta, C. B.; Baker, J. R., Jr. *J. Med. Chem.* **2005**, *48*, 5892–5899.
(17) Yordanov, A. T.; Kobayashi, H.; English, S. J.; Reijnders, K.; Milenic, D.; Krishna, M. C.; Mitchell, J. B.; Brechbiel, M. W. *J. Mater. Chem.* **2003**, *13*, 1523–1525.

(18) Lartigue, M.-L.; Slany, M.; Caminade, A.-M.; Majoral, J.-P. *Chem.—Eur. J.* **1996**, *2*, 1417–1426.
(19) Newkome, G. R.; Yoo, K. S.; Hwang, S.-H.; Moorefield, C. N. *Tetrahedron* **2003**, *59*, 3955–3964.
(20) Mihov, G.; Scheppelmann, I.; Müllen, K. *J. Org. Chem.* **2004**, *69*, 8029–8037.
(21) Woller, E. K.; Cloninger, M. J. *Biomacromolecules* **2001**, *2*, 1052–1054.
(22) Shi, X.; Lesniak, W.; Islam, M. T.; Muñiz, M. C.; Balogh, L. P.; Baker, J. R., Jr. *Colloids Surf., A* **2006**, *272*, 139–150.
(23) Walter, E. D.; Sebby, K. B.; Usselman, R. J.; Singel, D. J.; Cloninger, M. J. *J. Phys. Chem. B* **2005**, *109*, 21532–21538.
(24) Han, H. J.; Sebby, K. B.; Singel, D. J.; Cloninger, M. J. *Macromolecules* **2007**, *40*, 3030–3033.
(25) Suek, N. W.; Lamm, M. H. *Macromolecules* **2006**, *39*, 4247–4255.
(26) Lee, H.; Baker, J. R., Jr.; Larson, R. G. *J. Phys. Chem. B* **2006**, *110*, 4014–4019.
(27) Denkewalter, R. G.; Kolc, J.; Lukasavage, W. J. Macromolecular highly branched homogeneous compound based on lysine units. U.S. Patent 4,289,872, **1981**.
(28) Denkewalter, R. G.; Kolc, J. F.; Lukasavage, W. J. Macromolecular Highly Branched Homogeneous Compound. U.S. Patent 4,410,688, **1983**.
(29) Tam, J. P. *Proc. Natl. Acad. Sci. U.S.A.* **1988**, *85*, 5409–5413.
(30) Baigude, H.; Katsuraya, K.; Okuyama, K.; Yachi, Y.; Sato, S.; Uryu, T. *J. Polym. Sci., Part A: Polym. Chem.* **2002**, *40*, 3622–3633.
(31) Baigude, H.; Katsuraya, K.; Okuyama, K.; Kariya, N.; Uryu, T. *Sen'i Gakkaishi* **2004**, *60*, 118–124.
(32) Kaneshiro, T. L.; Wang, X.; Lu, Z.-R. *Mol. Pharm.* **2007**, *4*, 759–768.
(33) Bourne, N.; Stanberry, L. R.; Kern, E. R.; Holan, G.; Matthews, B.; Bernstein, D. I. *Antimicrob. Agents Chemother.* **2000**, *44*, 2471–2474.
(34) Matthews, B. R.; Holan, G.; Giannis, M. P. Agents for the Prevention and Treatment of Sexually Transmitted Diseases - II. Int. Patent WO 2002/079298, **2002**.
(35) Matthews, B. R.; Holan, G.; Karellas, P.; Henderson, S. A.; O'Keefe, D. F. Agent for the Prevention and Treatment of Sexually Transmitted Diseases - I. Int. Patent WO 2002/079299, **2002**.
(36) Tam, J. P. Multiple antigen peptide system. U.S. Patent 5,229,490, **1993**.
(37) Krippner, G. Y.; Lichti, G.; Razzino, P.; Kelly, B. D.; Pallich, S.; Henderson, S. A.; Scheppokat, A. M.; Williams, C. C.; Porter, C. J. H.; Boyd, B. J.; Kaminskas, L. M.; Rendle, P. M.; Greatrex, B. W. Macromolecular Compounds Having Controlled Stoichiometry. Int. Patent WO 2007/048190 A1, **2007**.
(38) Adamczyk, M.; Fishpaugh, J.; Mattingly, P. G.; Shreder, K. *Bioorg. Med. Chem. Lett.* **1998**, *8*, 3595–3598.
(39) Kim, C.; Kim, K. T.; Chang, Y.; Song, H. H.; Cho, T.-Y.; Jeon, H.-J. *J. Am. Chem. Soc.* **2001**, *123*, 5586–5587.
(40) Chang, Y.; Park, C.; Kim, K. T.; Kim, C. *Langmuir* **2005**, *21*, 4334–4339.
(41) Llinares, M.; Roy, R. *Chem. Commun.* **1997**, 2119–2120.
(42) Wender, P. A.; Kreider, E.; Pelkey, E. T.; Rothbard, J.; VanDeusen, C. L. *Org. Lett.* **2005**, *7*, 4815–4818.
(43) Krippner, G. Y.; Williams, C. C.; Kelly, B. D.; Henderson, S. A.; Wu, Z.; Razzino, P. Targeted Polylysine Dendrimer Therapeutic Agent. Int. Patent WO 2008/017125, **2008**.
(44) Roberts, B. P.; Scanlon, M. J.; Krippner, G. Y.; Chalmers, D. K. *Macromolecules* **2009**, *42*, 2775−2783.
(45) Chalmers, D. K.; Roberts, B. P. Silico: A Perl Molecular Toolkit, http://silico.sourceforge.net. Accessed June 9, 2008.
(46) Tripos SYBYL, St. Louis, MO, **2007**.
(47) Clark, M.; Cramer, R. D., III; van Opdenbosch, N. *J. Comput. Chem.* **1989**, *10*, 982–1012.
(48) Jorgensen, W. L.; Maxwell, D. S.; Tirado-Rives, J. *J. Am. Chem. Soc.* **1996**, *118*, 11225–11236.
(49) Damm, W.; Frontera, A.; Tirado-Rives, J.; Jorgensen, W. L. *J. Comput. Chem.* **1997**, *18*, 1955–1970.
(50) Jorgensen, W. L.; McDonald, N. A. *J. Mol. Struct. (THEOCHEM)* **1998**, *424*, 145–155.
(51) McDonald, N. A.; Jorgensen, W. L. *J. Phys. Chem. B* **1998**, *102*, 8049–8059.
(52) Rizzo, R. C.; Jorgensen, W. L. *J. Am. Chem. Soc.* **1999**, *121*, 4827–4836.
(53) Price, M. L. P.; Ostrovsky, D.; Jorgensen, W. L. *J. Comput. Chem.* **2001**, *22*, 1340–1352.
(54) Watkins, E. K.; Jorgensen, W. L. *J. Phys. Chem. A* **2001**, *105*, 4118–4125.
(55) Frisch, M. J.; Trucks, G. W.; Schlegel, H. B.; Scuseria, G. E.; Robb, M. A.; Cheeseman, J. R.; Zakrzewski, V. G.; Montgomery, J. A., Jr.; Stratmann, R. E.; Burant, J. C.; Dapprich, S.; Millam, J. M.; Daniels, A. D.; Kudin, K. N.; Strain, M. C.; Farkas, O.; Tomasi, J.; Barone, V.; Cossi, M.; Cammi, R.; Mennucci, B.; Pomelli, C.; Adamo, C.; Clifford, S.; Ochterski, J.; Petersson, G. A.; Ayala, P. Y.; Cui, Q.; Morokuma, K.; Malick, D. K.; Rabuck, A. D.; Raghavachari, K.; Foresman, J. B.; Cioslowski, J.; Ortiz, J. V.; Baboul, A. G.; Stefanov, B. B.; Liu, G.; Liashenko, A.; Piskorz, P.; Komaromi, I.; Gomperts, R.; Martin, R. L.; Fox, D. J.; Keith, T.; Al-Laham, M. A.; Peng, C. Y.; Nanayakkara, A.; Gonzalez, C.; Challacombe, M.; Gill, P. M. W.; Johnson, B.; Chen, W.; Wong, M. W.; Andres, J. L.; Gonzalez, C.; Head-Gordon, M.; Replogle, E. S.; Pople, J. A. *Gaussian 98*, Revision A.7; Gaussian, Inc.: Pittsburgh, PA, 1998.
(56) Jorgensen, W. L.; Chandrasekhar, J.; Madura, J. D.; Impey, R. W.; Klein, M. L. *J. Chem. Phys.* **1983**, *79* (2), 926–935.
(57) Kalé, L.; Skeel, R.; Bhandarkar, M.; Brunner, R.; Gursoy, A.; Krawetz, N.; Phillips, J.; Shinozaki, A.; Varadarajan, K.; Schulten, K. *J. Comput. Phys.* **1999**, *151*, 283–312.
(58) Phillips, J. C.; Braun, R.; Wang, W.; Gumbart, J.; Tajkhorshid, E.; Villa, E.; Chipot, C.; Skeel, R. D.; Kalé, L.; Schulten, K. *J. Comput. Chem.* **2005**, *26*, 1781–1802.
(59) Humphrey, W.; Dalke, A.; Schulten, K. *J. Mol. Graphics* **1996**, *14*, 33–38.
(60) DeLano, W. L. The PyMOL Molecular Graphics System, http://pymol.sourceforge.net. Accessed June 1, 2008.
(61) Hubbard, S. J.; Thornton, J. M. *NACCESS*, London, UK, 1993.
(62) Rudnick, J.; Gaspari, G. *J. Phys. A: Math. Gen.* **1986**, *19*, L191–L193.
(63) Dagnall, S. P.; Hague, D. N.; McAdam, M. E. *J. Chem. Soc., Perkin Trans. 2* **1984**, 1111–1114.
(64) Rissanou, A. N.; Economou, I. G.; Panagiotopoulos, A. Z. *Macromolecules* **2006**, *39*, 6298–6305.
(65) Welch, P.; Muthukumar, M. *Macromolecules* **1998**, *31*, 5892–5897.
(66) Lee, I.; Athey, B. D.; Wetzel, A. W.; Meixner, W.; Baker, J. R., Jr. *Macromolecules* **2002**, *35*, 4510–4520.
(67) Maiti, P. K.; Çağin, T.; Lin, S.-T.; Goddard, W. A., III *Macromolecules* **2005**, *38*, 979–991.
(68) Delort, E.; Nguyen-Trung, N.-Q.; Darbre, T.; Reymond, J.-L. *J. Org. Chem.* **2006**, *71*, 4468–4480.
(69) Epperson, J. D.; Ming, L. J.; Baker, G. R.; Newkome, G. R. *J. Am. Chem. Soc.* **2001**, *123* (35), 8583–8592.
(70) Woodbrey, J. C.; Rogers, M. T. *J. Am. Chem. Soc.* **1962**, *84*, 13–16.
(71) Gurtovenko, A. A.; Lyulin, S. V.; Karttunen, M.; Vattulainen, I. *J. Chem. Phys.* **2006**, *124*, 094904.

MA8021579